

## Comparative Numerical Analysis of NACA 2412, NACA 0012, and NACA 63-412 Airfoil Performance for Cessna 172 Aircraft Wings

*Md. Rafayet Bin Ali\*, Tammem Hasan*

Department of Mechanical Engineering, Rajshahi University of Engineering and Technology, Rajshahi-6204, Bangladesh

### ABSTRACT

This study investigates the impact of different wing profiles on the aerodynamic performance of the default NACA 2412 airfoil used in the Cessna 172 aircraft, along with two alternatives, NACA 0012 and NACA 63-412, through 3D flow analysis. All three airfoils were modeled in SolidWorks for numerical evaluation. Using ANSYS Fluent 2023R2, the aerodynamic characteristics, including the lift coefficient, drag coefficient, and lift-to-drag ratio, were analyzed across a range of angles of attack from 0 ° to 20 ° at a Reynolds number of  $R_e = 2.5 \times 10^5$ . Simulations were conducted using the k-epsilon turbulence model, revealing that the lift coefficient ( $C_l$ ) increased for all profiles with the angle of attack until it reached the stall point, which occurred at approximately 14 °. Among the profiles, NACA 63-412 achieved the highest lift coefficient, while NACA 0012 had the lowest. In terms of lift-to-drag (L/D) ratio, all profiles initially showed an increase up to around 4-6 degrees of attack before declining. Although NACA 63-412 initially maintained a higher L/D ratio, it experienced a steeper decline beyond this range compared to NACA 2412. At lower angles of attack, NACA 63-412 performed best, NACA 2412 showed better results at higher angles, and NACA 0012 showed poor results throughout. The NACA 63-412's high lift characteristics provide benefits in certain circumstances, even though the NACA 2412 is the standard airfoil for the Cessna 172-R due to its dependable, well-rounded performance.

Keywords: Cessna 172, Airfoil, 3d Simulation, k-  $\epsilon$  Model, Lift-to-Drag ratio



Copyright @ All authors

This work is licensed under a [Creative Commons Attribution 4.0 International License](https://creativecommons.org/licenses/by/4.0/).

### 1. Introduction

Aerodynamics is an area of study that examines the flow of air relative to the body. The effectiveness of any aerodynamic structure is significantly influenced by the properties and design of the airfoil used. The cross-sectional shape of a body placed in an air stream to produce an aerodynamic force as effectively as feasible is called an airfoil.[1]. The airflow over airfoils is a critical factor to consider when designing aircraft, missiles, sports vehicles, or any other aerodynamic objects[2]. When air moves over an aerodynamic surface, it creates two perpendicular forces, known as lift, acting perpendicular to the airflow, while the other drag, aligns with the direction of the flow. The primary focus in studying and designing an airfoil is to maximize lift while minimizing drag optimally. The creation of lift and drag is significantly influenced by the free-stream velocity at a fixed angle of attack ( $\alpha$ ). Up until a certain point, the lift-to-drag (L/D) ratio rises with increasing free-stream velocity at a certain angle of attack. Subsequently, it decreases as the velocity continues to increase. Up to a certain point, lift rises as the angle of attack ( $\alpha$ ) does. Beyond this critical angle, the flow begins to separate from the airfoil's upper surface, forming a large wake of stagnant air behind it. This flow separation, influenced by viscous effects, leads to a sharp drop in lift and a significant rise in drag. When this occurs, the airfoil is considered stalled, marking what is known as the stalling point [3]. The aerodynamic properties of an airfoil can be evaluated experimentally or via computational fluid dynamics (CFD), which uses numerical techniques, mathematical modeling, and specialized software tools to

forecast fluid flow. The NACA database, established by NASA's predecessor, the National Advisory Committee for Aeronautics, provides a wide range of airfoil designs that are commonly used in CFD modeling. The Cessna-172 aircraft utilizes an NACA 2412 airfoil. Sarker et al. [4] conducted a numerical study on an airfoil model of NACA 2412 to examine the effects of high Reynolds number flow on pressure and velocity distributions and aerodynamic forces, while varying the angle of attack in a SST Turbulence Model. Bacha et al. [5] developed a reliable and precise transition model from laminar to turbulent flow, integrating it into a CFD solver to improve drag prediction accuracy for two-dimensional airfoil transitional flow. Eleni et al.[6] analyzed the flow over an NACA 0012 airfoil at different angles of attack using a variety of turbulence models and a Reynolds number of  $3 \times 10^6$ , focusing on the impact of these factors on aerodynamic performance, including lift, drag, and flow separation. A. Meku et al. [7] investigated the wing design modifications that impacted the performance of the Cessna 172-R aircraft by experimental and numerical methods. They analyzed two alternative configurations: one with an extended span while retaining the original chord length and another with an increased chord length while maintaining the original span. M. Özdemir et al.[8] developed an interdisciplinary, multi-level design approach tailored for fixed-wing aircraft, illustrating its application through the design and optimization of the Cessna 172 N. Their work details the use of a newly created aircraft design tool, emphasizing streamlined and efficient design processes. Hüdayim Başak et al. [9] investigated how wing cross-

section and 3D airfoil shapes influence aerodynamic performance using numerical methods. Employing a biomimetic design approach, they developed new wing designs inspired by the wing structures of various bird species to enhance aerodynamic efficiency. Ü. Korkmaz et al.[10] analyzed the aerodynamic performance of the NACA 63-215 airfoil by examining its behavior across different angles of attack using CFD analysis.

Extensive research exists on the performance analysis of individual wing profiles; however, comparative studies of different wing profiles in practical applications remain limited. This study presents a numerical investigation comparing three wing profiles—NACA 2412, NACA 0012, and NACA 63-412—on the Cessna 172 model aircraft. Using the Standard k- $\epsilon$  model in ANSYS Fluent, we evaluated the aerodynamic characteristics of each profile to identify the most suitable airfoil for the aircraft.

## 2.Numerical Methodology:

### 2.1 Computational Methodology:

The steady-state RANS equations can be expressed as: Continuity Equation (Mass Conservation):

$$\frac{\partial}{\partial x_i}(\rho u_i) = 0 \quad (1)$$

Momentum equation:

$$\frac{\partial}{\partial x_j}(\rho u_i u_j) = -\frac{\partial}{\partial x_i}(p) + \frac{\partial}{\partial x_j} \left[ \mu \left( \frac{\partial u_i}{\partial x_j} + \frac{\partial u_j}{\partial x_i} - \frac{2}{3} \delta_{ij} \frac{\partial u_k}{\partial x_k} \right) \right] + \frac{\partial}{\partial x_j} (-\rho \overline{u_i' u_j'}) \quad (2)$$

The final term  $-\rho \overline{u_i' u_j'}$  is the Reynolds stress term, which arises from the turbulent fluctuations and represents additional stress due to turbulence. This nonlinear term in RANS equation can be solved by different turbulence models. Standard k- $\epsilon$  Model, was used.

### 2.2 Standard k- $\epsilon$ model:

The standard k- $\epsilon$  model in ANSYS Fluent falls into the two-equation turbulence models that provide the capability to determine both turbulent length and time scales by solving a pair of distinct transport and has been widely adopted in practical engineering flow simulations since its introduction by Launder and Spalding. Its popularity in industrial flow and heat transfer simulations stems from its robustness, cost-effectiveness, and reasonable accuracy across various turbulent flow scenarios. The standard k- $\epsilon$  model is based on transport equations for turbulence kinetic energy (k) and its dissipation rate ( $\epsilon$ )[11].

$$\frac{\partial}{\partial t}(\rho k) + \frac{\partial}{\partial x_i}(\rho k u_i) = \frac{\partial}{\partial x_j} \left[ \left( \mu + \frac{\mu_t}{\sigma_k} \right) \frac{\partial k}{\partial x_j} \right] + G_k + G_b - \rho \epsilon - Y_{M+} S_k \quad (3)$$

$$\frac{\partial}{\partial t}(\rho \epsilon) + \frac{\partial}{\partial x_i}(\rho \epsilon u_i) = \frac{\partial}{\partial x_j} \left[ \left( \mu + \frac{\mu_t}{\sigma_\epsilon} \right) \frac{\partial \epsilon}{\partial x_j} \right] + C_{1\epsilon} \frac{\epsilon}{k} (G_k + C_{3\epsilon} G_b) - C_{2\epsilon} \rho \frac{\epsilon^2}{k} + S_\epsilon \quad (4)$$

In these equations,  $G_k$  and  $G_b$  represent turbulence kinetic energy generation due to velocity gradients and buoyancy, respectively, while  $Y_M$  accounts for compressibility effects. Constants  $C_{1\epsilon}$ ,  $C_{2\epsilon}$  and  $C_{3\epsilon}$ , along with turbulent Prandtl numbers  $\sigma_k$  and  $\sigma_\epsilon$ , control energy and dissipation rates, with  $S_k$  and  $S_\epsilon$  as user-defined source terms.

### 2.3 Geometry:

To plot the profiles of NACA 2412, NACA 0012, and NACA 63-412, coordinates were obtained from an online profile generator [12]. The 3D model was then created using SolidWorks software.



**Fig.1** CAD model of the NACA 2412 airfoil in SolidWorks



**Fig.2** CAD model of the NACA 0012 airfoil in SolidWorks

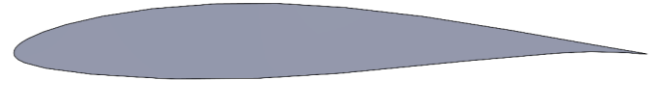


**Fig.3** CAD model of the NACA 63-412 airfoil in SolidWorks

Figures 1, 2, and 3 present various 3D airfoil models displayed in a 2D view. Table 1 lists the half-wing input parameters for the Cessna 172-R aircraft, and the dimensions are the same for all three airfoils.

**Table 1** Data for the half-wing configurations

Parameter	Actual	Model
Half wingspan (m)	5.5000	0.2500
Length of root chord (m)	1.4730	0.0670
Length of tip chord (m)	1.4730	0.0670

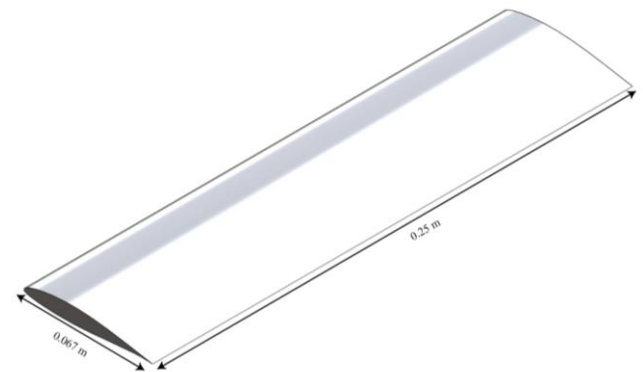


**Fig.4** 3D model of NACA 63-412 with different dimensions

### 2.4 Computational Domain:

The geometry was then imported to ANSYS design modeler where the whole fluid domain was divided into 3 regions.

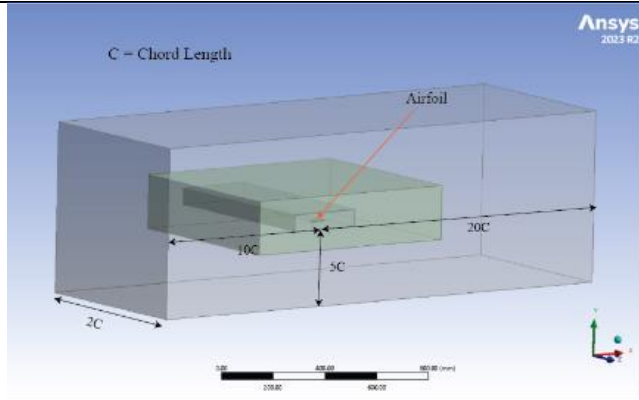


**Fig.5** Computational domains.

From Fig 5, it is seen that coarser mesh was applied in the distant region, while finer mesh was used in the body of influence around the airfoil. Maximum skewness was kept under 0.9. Mesh elements for every model were around 2.8 million.

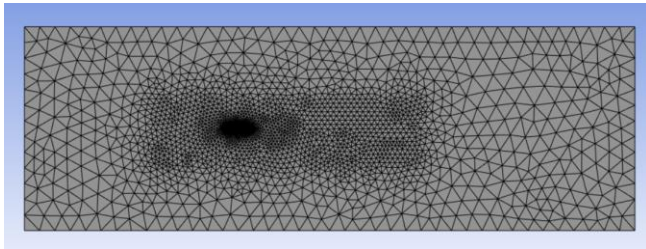


**Fig.6** Mesh in all the fluid domain

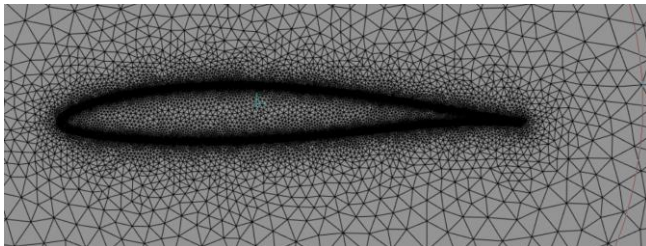


**Fig.7** Mesh around the airfoil

**Table 2** Inflation layer details

Inflation First layer Thickness	No of Layers	Inflation Growth rate
0.32mm	5	1.2

#### 2.4 Boundary Conditions

The problem involves airflow around three airfoils at different angles of attack (0–20 degrees). Table 3 presents the inputs and boundary conditions.

**Table 3** Boundary conditions and inputs

Type	Pressure based
Models	Standard K-epsilon
Fluid	Air
Density	1.225 kg/m <sup>3</sup>
Viscosity	1.7894e-05 kg/m. s
Inlet Velocity	55.558 m/s
Initial Pressure	0 Pa
Reynolds Number	2.5×10 <sup>5</sup>
Temperature	288.16 K
Residuals	0.00001

A coupled solver was used for simulation. A second-order upwind spatial discretization method was used to solve all the equations (pressure, momentum, and turbulence) to improve the accuracy of capturing flow characteristics. A least-squares cell-based method was used to compute gradients to increase the accuracy of changes between cells.

#### 3. Validation:

For model validation, the numerical data for the NACA 2412 airfoil is compared with the experimental results from Addisu Alamirew Meku et al.[13], conducted at the same Reynolds number. As shown in Table 4, the deviations between experimental and numerical values are under 15%. Consequently, a similar setup is used for the numerical simulation of the NACA 0012 and NACA 63–412 airfoils.

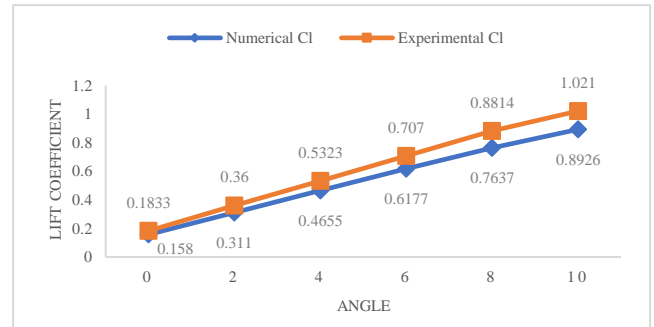


**Fig.8** A comparison between the Experimental and Numerical lift Coefficient

**Table 4** Calculation of deviation

Angle (degrees)	Numerical C <sub>L</sub>	Experimental C <sub>L</sub>	Deviation
0	0.158	0.1833	12.71%
2	0.311	0.36	13.61%
4	0.4655	0.5323	12.55%
6	0.6177	0.707	12.63%
8	0.7637	0.8814	13.35%
10	0.8926	1.021	12.06%

#### 4. Result and Discussion:

Figure 9 shows how the lift coefficient varies with variations in the angle of attack for three different airfoils: NACA 2412, NACA 63-412, and NACA 0012. From 0° to 20°, the angle of attack rises, each airfoil initially experiences a steady increase in lift coefficient. This increase continues until each airfoil reaches a maximum lift value, after which the lift coefficient begins to drop, indicating the onset of stall. Among the three airfoils, NACA 63-412 exhibits the highest overall lift coefficient, with a peak around 1.2 at approximately 16° angle of attack. This higher lift performance suggests that NACA 63-412 is well-suited for applications requiring greater lift at higher angles. The NACA 2412 airfoil follows closely, peaking at a lift coefficient just above 1.0, at approximately 14° AOA. Meanwhile, NACA 0012, a symmetric airfoil, generates the lowest lift among the three, with a peak lift coefficient of roughly 0.8, also approximately 14°.

Both NACA 2412 and NACA 0012 show a stall onset around 14° AOA, while NACA 63-412 demonstrates improved stall characteristics by stalling later at 16° AOA. This delayed stall in NACA 63-412 highlights its ability to maintain lift at higher angles before losing aerodynamic stability, making it

advantageous for scenarios that require sustained lift at larger attack angles.

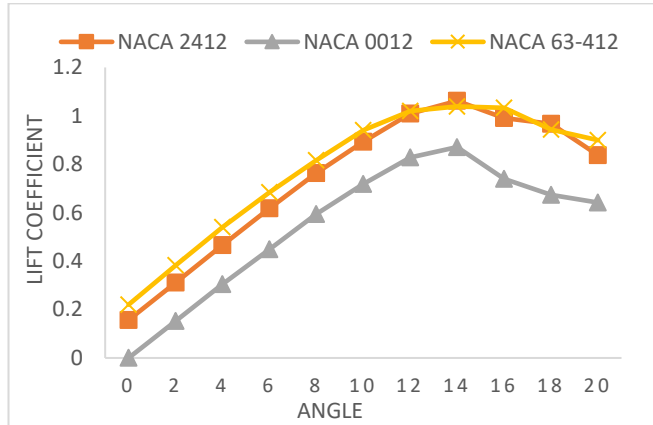


**Fig.9** Lift coefficient vs AOA for different airfoils

Fig. 10 demonstrates the relationship between the drag coefficient ( $C_d$ ) and the angle of attack (AOA) for the NACA 2412, NACA 0012, and NACA 63-412 airfoil designs. As the AOA increases from  $0^\circ$  to  $20^\circ$ , all three airfoils exhibit a gradual rise in drag coefficient, with a sharper increase at higher angles due to increased airflow resistance. NACA 63-412 consistently has the highest drag coefficient, reaching approximately 0.27 at  $20^\circ$  AOA, likely due to its cambered design that enhances lift but increases drag. NACA 2412 follows with a slightly lower drag coefficient of around 0.25 at  $20^\circ$  AOA, as it balances lift and drag with its moderate camber profile. NACA 0012, a symmetric design, has the lowest drag coefficient, reaching only about 0.23 at  $20^\circ$  AOA, as its shape minimizes drag, making it suitable for low-resistance conditions. This trend highlights the design focus of each airfoil, with NACA 63-412 prioritizing lift, NACA 0012 minimizing drag, and NACA 2412 balancing the two, reflecting aerodynamic trade-offs in airfoil design.

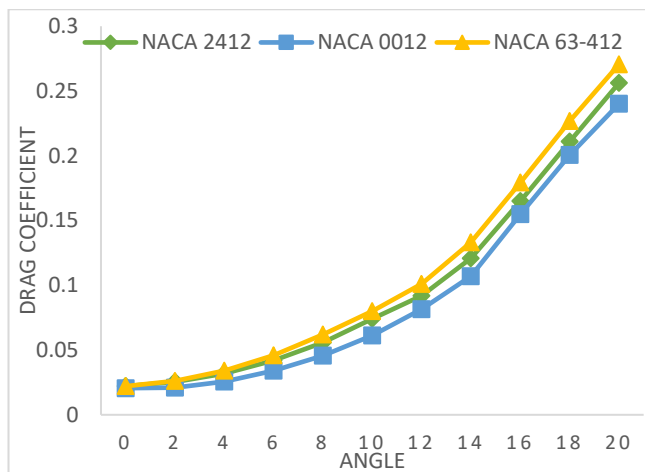


**Fig.10** Drag coefficient vs AOA for different airfoils.

Fig. 11 illustrates how the lift-to-drag ratio (L/D) and angle of attack (AOA) are related to three different airfoil designs: NACA 2412, NACA 0012, and NACA 63-412. The lift-to-drag ratio first increases for each airfoil as the AOA increases, reaching a peak before decreasing as the angle continues to grow. NACA 63-412 achieves the highest lift-to-drag ratio, peaking around 17 at approximately  $6^\circ$  AOA, indicating strong lift performance relative to drag at this

angle. NACA 2412 follows closely, with a maximum lift-to-drag ratio near 15 around  $8^\circ$  AOA. NACA 0012, a symmetric airfoil, reaches a peak L/D ratio of about 13 at  $6^\circ$  AOA. Beyond these peak points, all three airfoils experience a decline in L/D ratio as drag increases with angle, demonstrating reduced aerodynamic efficiency. This trend reflects each airfoil's aerodynamic characteristics: NACA 63-412 shows superior lift relative to drag at moderate angles, NACA 2412 maintains a balanced performance, and NACA 0012 demonstrates efficient drag reduction at low angles but lower peak lift-to-drag performance.

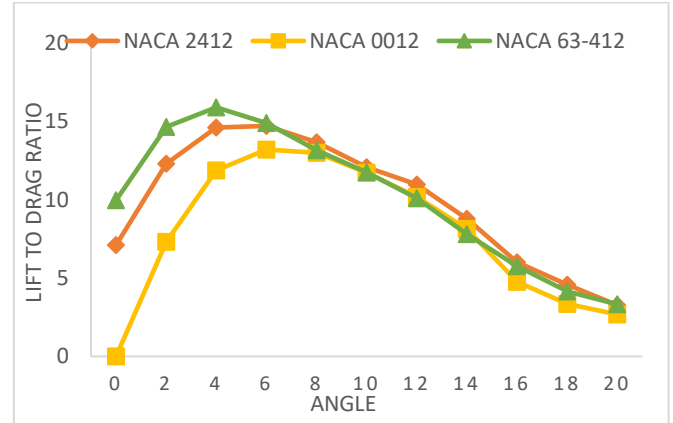


**Fig.11** L/D ratio vs Angle

#### 4.1 Pressure and Velocity contour:

Figures 12, 13, and 14 show three distinct airfoil pressure profiles at different angles of attack, all at the same Reynolds number.

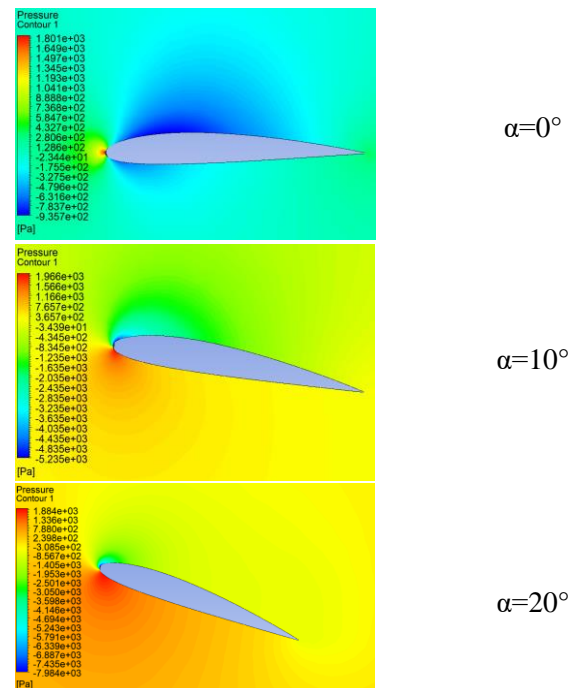


**Fig.12** Pressure Contours for NACA 2412

It shows that the airfoil's lower surface has more pressure than its upper surface. Additionally, a region of negative pressure spans the entire upper surface of each airfoil. Pressure on the bottom surface increases as the angle of attack increases, while the upper surface pressure decreases further. This pressure distribution generates a lift on the

airfoil. As the angle of attack increases, the pressure differential between the lower and higher surfaces keeps growing until stall or flow separation occurs on the upper surface.

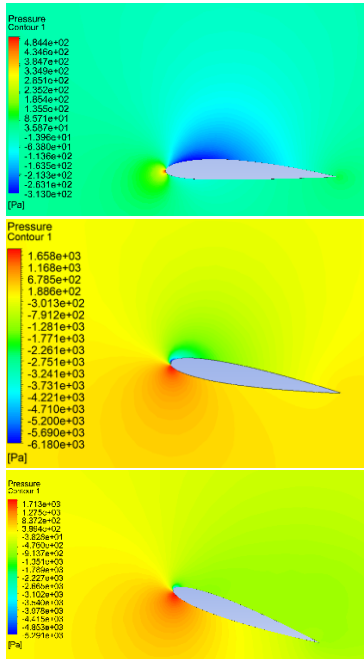


**Fig.13** Pressure Contours for NACA 0012

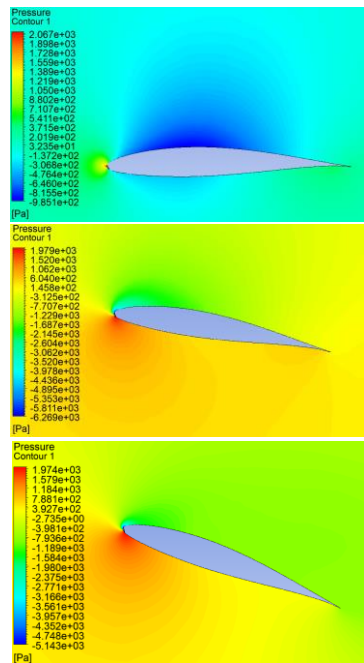


**Fig.14** Pressure Contours for NACA 63-412

Figures 15, 16, and 17 show the airfoil's upper surface exhibits higher velocity than its lower surface. Airflow stays connected to the airfoil's surface at lower angles of attack. The velocity contours show that flow separation starts at the trailing edge and progressively advances toward the leading edge with further increases as the angle of attack rises. After a while, the lift coefficient decreases because of this flow separation at greater angles of attack.

There is a low-velocity area on the lower side and a high-velocity acceleration area on the upper side due to the stagnation points moving slightly toward the trailing edge

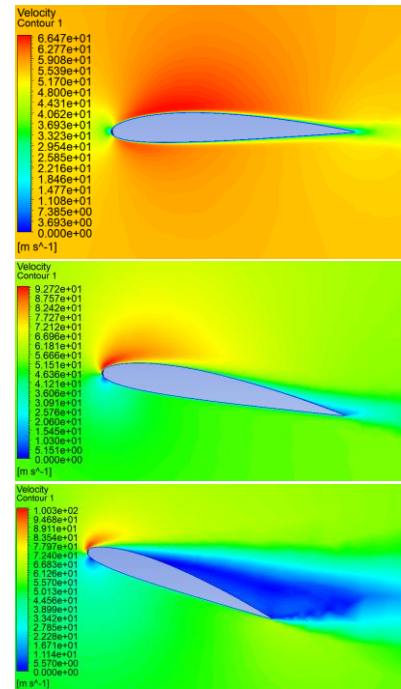
along the lower surface from an angle of attack of 5 degrees. This causes the upper surface to have less pressure and the lower surface to have more pressure, in accordance with Bernoulli's principle. Consequently, both the lift coefficient and drag coefficient increase, but after reaching a critical angle, lift decreases due to stall while drag continues to increase.

In a symmetrical airfoil, such as the NACA 0012, the velocity and pressure distributions on both surfaces would match at zero incidence, resulting in zero net lift. However, since the NACA 2412 and NACA 63-412 are non-symmetrical airfoils, the pressure and velocity distributions differ between the two surfaces, creating lift even at zero incidence.

$\alpha=0^\circ$

$\alpha=10^\circ$

$\alpha=20^\circ$

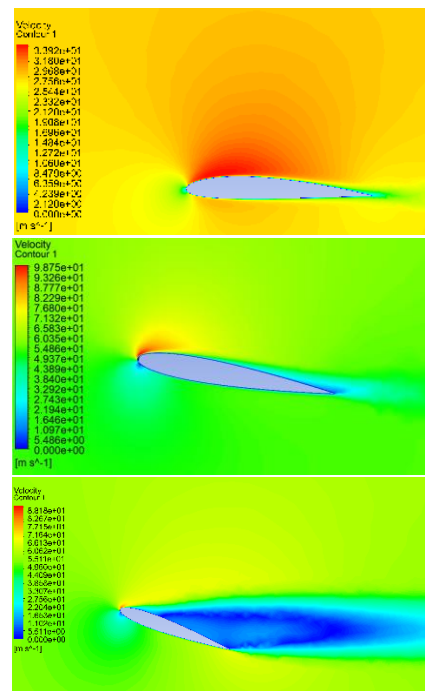


$\alpha=0^\circ$

$\alpha=10^\circ$

$\alpha=20^\circ$

**Fig.15** Velocity Contours for NACA 2412



$\alpha=0^\circ$

$\alpha=10^\circ$

$\alpha=20^\circ$

**Fig.16** Velocity Contours for NACA 0012

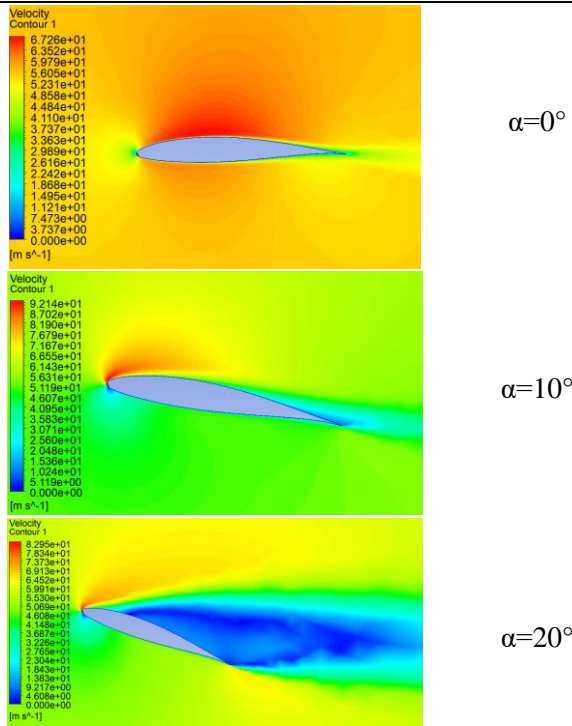


**Fig.17** Velocity Contours for NACA 63-412

## 5. Conclusion

This study's objective is to contrast different airfoils with the standard NACA 2412 airfoil for the Cessna 172-R aircraft. The selected airfoils include the NACA 0012 and NACA 63-412. Numerical analysis reveals that:

1. NACA 63-412 generally produces a higher lift coefficient than the other airfoils, though its drag coefficient is comparatively higher.
2. Stalls occur earlier for NACA 2412 and NACA 0012, while it happens later for NACA 63-412.
3. The NACA 63-412 lift-to-drag ratio is superior at lower angles (up to 6 degrees) but then falls below NACA 2412, although it remains close.
4. NACA 0012 demonstrates the lowest overall performance, showing minimal drag across all angles but also generating less lift. Consequently, its lift-to-drag ratio is the lowest across all angles.

From this study it can be said that while the NACA 2412 airfoil is the standard choice for the Cessna 172-R due to its balanced performance and proven reliability, the NACA 63-412's high lift characteristics offer advantages in specific situations.

## References

- [1] M. Kevadiya and H. A. Vaidya, "2D Analysis of Naca 4412 Airfoil," *International Journal of Innovative Research in Science, Engineering and Technology*, vol. 2, no. 5, pp. 1686–1691, 2013.

- [2] MD. S. H., "a Comparative Flow Analysis of Naca 6409 and Naca 4412 Aerofoil," *International Journal of Research in Engineering and Technology*, vol. 03, no. 10, pp. 342–350, 2014.
- [3] J. D. Anderson, *Fundamentals of Aerodynamics* (6th edition), vol. 1984, no. 3, 2011.
- [4] S. Sarkar and S. B. Mughal, "in CFD Analysis of Effect of Flow over NACA 2412 Airfoil through the Shear Stress Transport Turbulence Model CFD ANALYSIS OF EFFECT OF FLOW OVER NACA 2412 AIRFOIL THROUGH THE SHEAR STRESS TRANSPORT TURBULENCE MODEL," *International Journal of Mechanical And Production Engineering*, no. 5, pp. 2320–2092, 2017.
- [5] W. A. Bacha and W. S. Ghaly, "Drag prediction in transitional flow over two-dimensional airfoils," *Collection of Technical Papers - 44th AIAA Aerospace Sciences Meeting*, vol. 5, no. January, pp. 2999–3017, 2006.
- [6] E. Douvi, T. Athanasios, and D. Margaritis, "Evaluation of the turbulence models for the simulation of the flow over a National Advisory Committee for Aeronautics (NACA) 0012 airfoil," *Journal of Mechanical Engineering Research*, vol. 4, 2012.
- [7] A. A. Meku and D. K. N. Rao, "Analytical and Experimental Studies on Modified Wing Configurations of Cessna 172-R Aircraft to Improve Performance," *Journal of Aerospace Engineering*, vol. 37, no. 3, 2024.
- [8] M. Özdemir and D. F. Kurtuluş, "Model based aircraft design and optimization: a case study with cessna 172N aircraft," *Engineering Research Express*, vol. 5, no. 3, 2023.
- [9] H. BASAK and A. Akdemir, "Design Optimization of Cessna 172 Wing With Biomimetic Design Approach," *International Journal of Pioneering Technology and Engineering*, vol. 3, no. 01, pp. 07–15, 2024.
- [10] Ü. Korkmaz, İ. Göv, and M. H. Doğru, "Aerodynamic Analyses of Naca 63-215," *The International Journal of Energy & Engineering Sciences*, vol. 2020, no. 2, pp. 156–166, 2020.
- [11] "ANSYS Fluent Theory Guide 15 | PDF | Fluid Dynamics | Fluid Mechanics." Accessed: Oct. 29, 2024.[Online].Available:<https://www.scribd.com/document/556513357/ANSYS-Fluent-TheoryGuide-15>
- [12] "Airfoil plotter (n63412-il)." Accessed: Oct. 30, 2024.[Online].Available:<http://airfoiltools.com/plotter/index>
- [13] A. A. Meku and D. K. N. Rao, "Analytical and Experimental Studies on Modified Wing Configurations of Cessna 172-R Aircraft to Improve Performance," *Journal of Aerospace Engineering*, vol. 37, no. 3, May 2024.

## NOMENCLATURE

- $C_l$  : co-efficient of lift  
 $AoA$  : Attack of angle, Degree  
 $C_d$  : co-efficient of drag  
 $L/D$  : Lift to drag ratio  
 $\alpha$  : Angle of attack